

# Electric Fields and Large-Scale Undulations in the Evening Sector of the Diffuse Auroral Zone

D. G. Baishev<sup>a</sup>, E. S. Barkova<sup>a</sup>, A. E. Stepanov<sup>a</sup>, F. Rich<sup>b</sup>, and K. Yumoto<sup>c</sup>

<sup>a</sup>Yu.G. Shafer Institute of Cosmophysical Research and Aeronomy, Siberian Branch, Russian Academy of Sciences,  
pr. Lenina 31, Yakutsk, 677980 Russia

<sup>b</sup>Air Force Research Laboratory, Hanscom Air Force Base, Massachusetts, USA

<sup>c</sup>Space Environment Research Center, Kyushu University, Fukuoka, Japan

e-mail: [baishev@ikfia.ysn.ru](mailto:baishev@ikfia.ysn.ru)

Received April 14, 2009; in final form, July 8, 2009

**Abstract**—The synchronous observations of strong electric fields and large-scale undulations observed on December 12, 2004, in the evening sector of the diffuse auroral zone 0900–1000 UT ( $\sim$ 1700–1800 MLT) have been analyzed. The appearance of strong northward electric field at  $\sim$ 0900 UT was almost simultaneously registered at Tixie Bay ionospheric station ( $71.6^\circ$  N,  $128.9^\circ$  E,  $L = 5.6$ ) and on the DMSP F15 satellite. At 0910–1000 UT, the all-sky TV camera at Tixie Bay and the DMSP satellites (F13, F14, and F15) registered eight undulations propagating westward at a velocity of 0.7–0.8 km/s. The undulation parameters registered during the TV observations agree with the satellite measurements. The distinctive feature of the analyzed event consists in that an intense electric field and undulations were localized within the diffuse zone in the region of increased precipitation of keV electrons. A comparison of the ground-based and satellite measurements made it possible to draw the conclusion on the necessary conditions for formation of diffuse undulations.

**DOI:** [10.1134/S0016793210010056](https://doi.org/10.1134/S0016793210010056)

## 1. INTRODUCTION

Large-scale undulations were for the first time detected in the DMSP photographs [Lui et al., 1982]. Undulations with amplitudes of 40–400 km and wavelengths of  $\sim$ 200–900 km were observed at the equatorward boundary of diffuse auroras ( $\Phi' \sim 60^\circ$ ) in the evening sector near the ring current maximum. According to [Kelley, 1986], the undulations originate as a result of development of the Kelvin–Helmholtz instability, caused by the generation of intense electric fields directed poleward and localized equatorward of auroral electron precipitation.

The origination of subauroral polarization streams (SAPSs) [Foster and Burke, 2002] is one of the vivid manifestations of intense electric fields in the region of the main ionospheric trough. Foster and Vo [2002] studied the SAPS morphology and characteristics based on the data of the Millstone Hill incoherent scatter radar for 1979–2000. They indicated that such streams are registered from evening to early morning hours at  $K_p > 4$ . In the premidnight sector the polarization stream is observed equatorward of  $L = 4$  occupying latitudes of  $3^\circ$ – $5^\circ$  and has a maximal velocity of  $>900$  m/s.

Several cases of large-scale undulations were registered with a GUVI instrument on the TIMED satellite [Zhang et al., 2005]. Large-scale undulations were observed at the equatorward boundary of diffuse pro-

ton aurora during magnetic storms ( $Dst < -60$  nT) on the dayside, nightside, and morning side. On the dayside, the undulations were accompanied by a considerable convective shift in the region of their observation. The synchronous DMSP and TIMED measurements during the periods when undulations were registered indicated that high drift velocities ( $>1000$  m/s) and their steep gradient along latitude ( $>0.1$  s $^{-1}$ ) are the necessary conditions for generation of large-scale undulations.

The aim of this work is to study the spatial–temporal dynamics and generation conditions of large-scale undulations registered in the evening sector on December 12, 2004 during the synchronous ground-based and satellite measurements.

## 2. ANALYSIS OF OBSERVATIONS

We analyzed the TV observations at Tixie Bay with a time resolution of  $\sim$ 4 s [Shiokawa et al., 1996], DMSP satellites, magnetic field variations measured in the scope of the CARISMA and CPMN projects, and ionospheric disturbances at Tixie Bay (Parus Russian ionospheric station) and Zhigansk (DPS-4 digisonde). The geomagnetic and geographic coordinates, international codes, and geomagnetic local time of the used stations are presented in table. The data on IMF were obtained from the GEOTAIL satel-

The list of the stations used in an analysis

Ser. no.	Station name	Code	Geographic coordinates		Geomagnetic coordinates		Local magnetic midnight (UT)
			latitude, deg	longitude, deg	latitude, deg	longitude, deg	
1	Kotelny	KTN	76.0	135.9	70.3	200.1	1553
2	Tixie Bay	TIX	71.6	128.9	66.1	197.7	1602
3	Zhigansk	ZGN	66.8	123.4	61.4	194.6	1613
4	Gillam	GILL	56.4	265.4	66.3	332.5	0634
5	Island Lake	ISLL	53.9	265.3	63.9	332.8	0633

lite (20.2, 21.9, 3.1)  $R_E$  in GSE coordinates. The disturbance propagation time from the satellite to the subsolar point was  $\sim 3$  min.

Figure 1 illustrates the geomagnetic conditions in the midnight and evening sectors from 0730 to 1100 UT on December 12, 2004. Figure 1 presents the IMF variations, auroral station magnetograms, and the variations in auroral luminosity in the north–south direction (a keogram) according to the TV camera data at Tixie Bay station (the lower panel). The keogram was constructed in the geographic latitude–universal time coordinates taking into account the altitude of auroras ( $\sim 110$  km). Figure 1 indicates that the  $B_z$  component oscillated from  $-3$  to  $3$  nT, and the IMF  $B_y$  values remained positive ( $\sim 5$  nT) during the entire considered period. The solar wind density measured by the ACE satellite at  $X = -240R_E$  was about  $14 \text{ cm}^{-3}$ , and the velocity was  $\sim 440 \text{ km/s}$  (not shown). Note that the  $Dst$  index was  $-43$  nT. The magnetic field variations at auroral stations testify to the development of the DP2 two-vortex current system and enhancement of convection at  $\sim 0730$ – $1000$  UT and to the substorm onset at  $\sim 1000$  UT. The intensities of the westward electrojet in the midnight sector (GILL and ISLL) and eastward electrojet in the evening sector (KTN and TIX) were comparable ( $\Delta H \sim 200$  nT). The variations in the diffuse luminosity equatorward boundary can be traced on the keogram. The keogram was dark because of cloudiness during the observation period. It is clear that the equatorward boundary moved southward (from  $\sim 74^\circ$  to  $\sim 71^\circ$ ) at a velocity of  $\sim 200 \text{ m/s}$  at 0830–0900 UT. The region of the maximal intensity of the eastward (westward) electrojet in the evening (midnight) sector moved synchronously with this boundary.

Eight undulations were registered with a TV camera at 0910–1000 UT. We should note that large-scale undulations were localized within the diffuse zone but the position of the diffuse aurora equatorward boundary remained unchanged ( $\sim 71^\circ$ ).

We now consider in more detail the dynamics of large-scale undulations. Figure 2 shows the keogram in the direction north–south (Fig. 1a) and the TV frames of the observed undulations (Fig. 1b). The neg-

ative TV frames of auroras are presented. The frames show a weak gray background owing to cloudiness; therefore, a discrete auroral arc located north of the Tixie Bay zenith and distinctly registered on the DMSP satellites (see Fig. 5) merges with wave-like structures on the keogram. Large-scale undulations were observed at geographic latitudes of  $74^\circ$ – $72.5^\circ$ , i.e., within the diffuse zone. The estimates indicated that the undulation amplitude varied from  $\sim 100$  to  $150$  km and the wavelength was  $\sim 200$ – $300$  km.

To determine the propagation velocities of undulations, we constructed the keogram in the direction east–west at a geographic latitude of  $73^\circ$  using the TV camera data (Fig. 3). Seven westward undulations are clearly defined on the keogram. The eighth undulation, localized at a latitude of  $\sim 72.5^\circ$  is not observed because the region of undulation formation is shifted southward. Undulations first propagated at a constant velocity of  $\sim 800 \text{ m/s}$ , and the velocity decreased to  $\sim 700 \text{ m/s}$  at the end of the analyzed interval.

The development of ionospheric disturbances at 0815–0900 UT is presented in Fig. 4 which presents the ionograms at Tixie Bay and Zhigansk stations. The data of vertical sounding at Tixie Bay indicated that this station was in the zone diffuse auroras and the ionogram at 0815 UT illustrates a typical pattern with diffuse traces of irregular reflections in the ionospheric  $F$  and  $E$  regions. At 0830 UT, a sporadic  $E_{sr}$  layer with a frequency of 2.7 MHz caused by high-energy proton precipitation was observed at Tixie Bay. A regular  $F$  layer with critical frequencies of 3.1 and 2.7 MHz was registered at Zhigansk at 0815 and 0830 UT, respectively. The absence of reflections from the  $E$  layer and a decrease in the  $foF2$  critical frequencies at Zhigansk indicate that the latter station was localized within the main ionospheric trough. At 0845, the critical frequency of the  $E_{sr}$  layer decreased to 2 MHz at Tixie Bay, and a diffuse irregular trace appeared in the  $F$  region. At Zhigansk the  $foF2$  critical frequency decreased to 2.0 MHz at that instant. Ionospheric absorption began at Zhigansk at 0900 UT. Beginning from 0900 UT, a sporadic trace ( $E_{sa}$ ) appeared at Tixie Bay which indicates that a discrete auroral arc appeared near the station zenith [Brunelli and Nam-

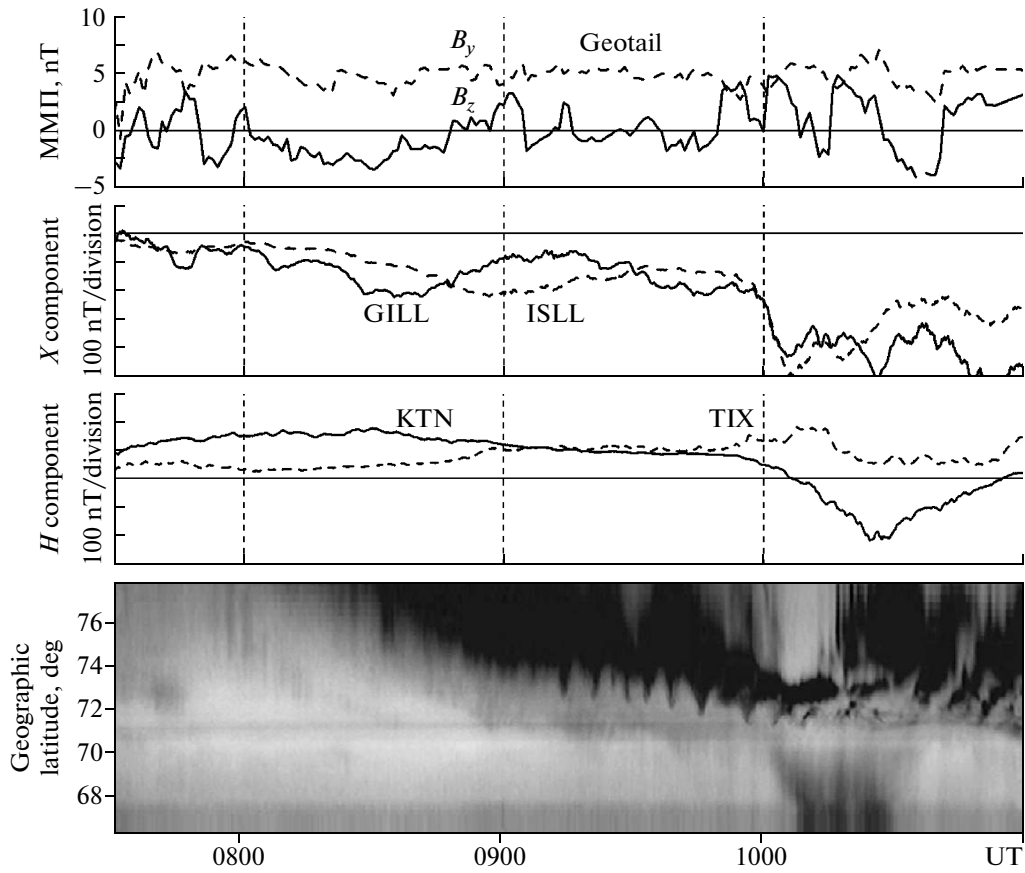


**Fig. 1.** From top to bottom: the variations in the  $B_y$  (a dashed line) and  $B_z$  (a solid line) components according to the Geotail satellite data; the variations in the magnetic field  $X(H)$  component at the auroral stations in the evening (KTN and TIX) and post-midnight (GILL and ISLL) sectors; and the keogram in the direction north–south at Tixie Bay for the event of December 12, 2004.

galadze, 1988]. A trace of the  $E_{ss}$  sporadic layer (slant  $E_s$ ) which indicated that a strong electric field appeared was also observed here [Olesen et al., 1986].

A successful pass of the DMSP satellites made it possible to obtain additional information about electric fields and particles and compare the dynamics and parameters of undulations on the Earth and satellite. The satellite data are presented in geographic coordinates in Fig. 5. The left-hand panels of Fig. 5 present the auroral photographs from the DMSP satellites: (a) F15, (b) F13, and (c) F14. The right-hand panels of Fig. 5 shows the spectrograms of electron and proton precipitation, the variations in the horizontal drift velocity  $V_y$  (a solid line), and the velocity gradient (a dotted line) measured on the DMSP satellites: (d) F15 and (e) F13. The gradient (shear according to the [Kelley, 1986] terminology) of the drift velocity ( $V_y$ ) was calculated along the satellite trajectory during the 5-min period. The scanning zone along the satellite pass is ~3000 km. The time shown on the photographs corresponds to the time when the satellite crossed the

region of undulation observation. The Tixie Bay (TIX) station position is marked by a cross.

The DMSP F15 satellite registered the formation of the first undulation at ~0910 UT (~1800 MLT) ~6° east of the TIX meridian (Fig. 5a); therefore, a TV camera at TIX registered this undulation at 0912–0915:35 UT (Fig. 2a). The undulation with an amplitude of ~150 km and a wavelength of ~250 km was localized within the diffuse zone which is related to precipitation of protons with an energy of >10 keV (Fig. 5d, ~0909–0911 UT).

Figure 5d indicates that the first increase in  $V_y$  at 0908:20–0909 UT was related to the subauroral polarization stream and was observed equatorward of the diffuse zone. The second increase in  $V_y$  related to the region of energetic proton precipitation began at 0909:10 UT, i.e., within the diffuse auroral zone. An abrupt increase in  $V_y$  which coincided with the instant of undulation formation (~0910 UT) was observed at 0910:10–0910:40 UT (marked by a gray rectangle). At that instant high azimuthal velocities were observed (185–850 m/s) and the  $V_y$  gradient varied in a wide

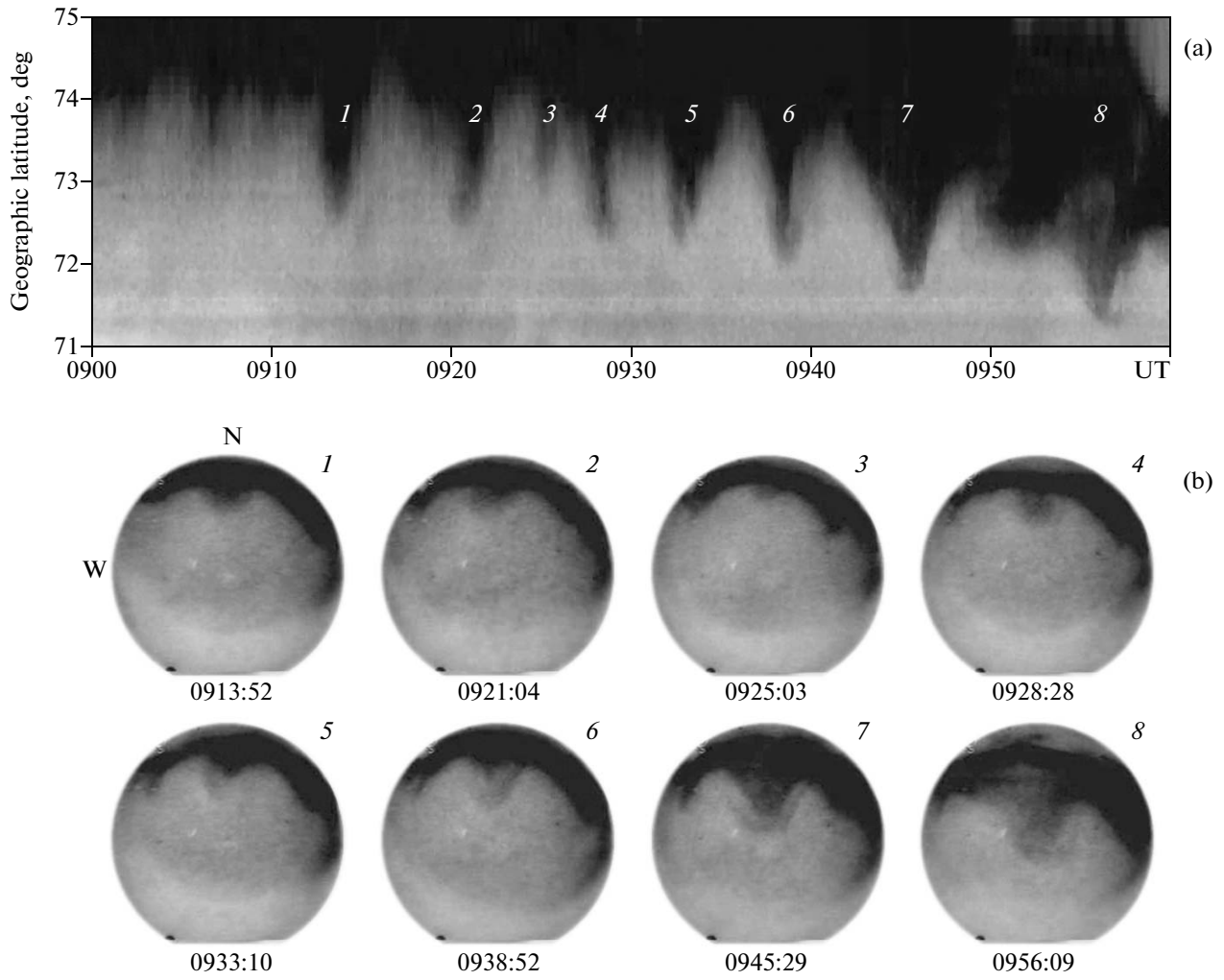


**Fig. 2.** The keogram in the direction north–south at 0900–1000 UT and the TV frames of auroras at Tixie Bay.

range (from  $-0.045$  to  $0.078 \text{ s}^{-1}$ ). We also note that precipitation of electrons with an energy of  $\sim 1 \text{ keV}$  increased by an order of magnitude at the latitude of

undulation registration (0910:25–0910:30 UT), and a trough is observed in precipitation of  $10 \text{ keV}$  protons (0910:25–0910:40 UT). A discrete arc caused by electron precipitation of the inverted- $V$  type (0910:55–0911:15 UT) was localized  $\sim 1^\circ$  north of the undulation formation region. Higher drift velocities were observed at that time.

Figures 5b and 5e show the DMSP F13 data at 0937–0942 UT ( $\sim 1700$  MLT). The satellite registered several undulations (Fig. 5b). As during the previous satellite pass, undulations with an amplitude of  $\sim 150 \text{ km}$  and a wavelength of  $\sim 300 \text{ km}$  were localized within the diffuse zone  $\sim 1^\circ$  south of a discrete auroral arc (Fig. 5b). Two maximums were observed in the drift velocity ( $V_y$ ) variations (Fig. 5e). The first velocity maximum ( $\sim 600 \text{ m/s}$ ) at 0937:50–0938:20 UT was observed outside the diffuse zone and was related to SAPS. The second maximum (0939:25–0939:50 UT) was registered within the diffuse zone and was characterized by lower velocities ( $\sim 500 \text{ m/s}$ ) and small  $V_y$

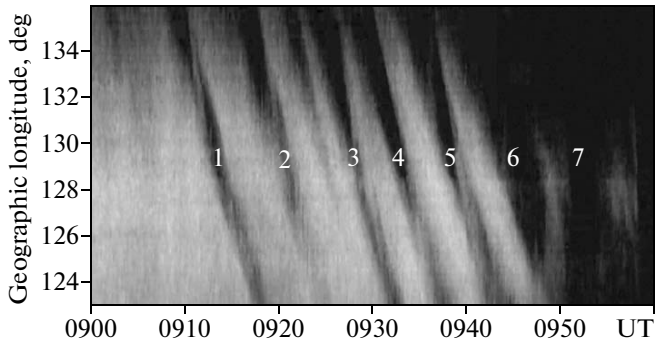


**Fig. 3.** The keogram in the direction east–west at 0900–1000 UT at a geographic latitude of  $73^\circ$ .

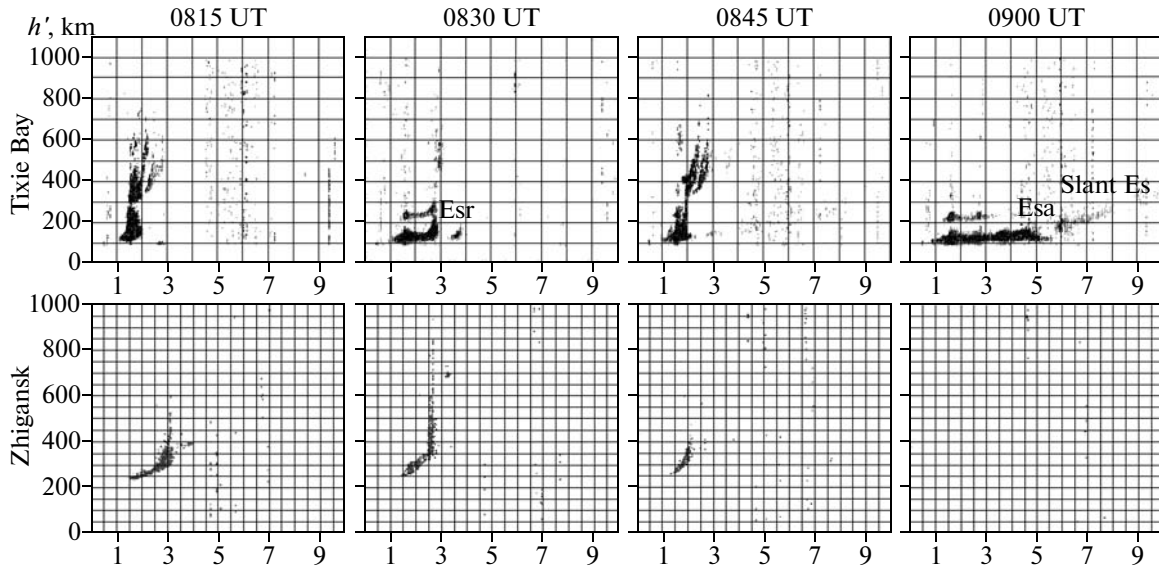


**Fig. 4.** The ionograms at Tixie Bay and Zhigansk stations at 0815–0900 UT.

gradients. Precipitation of high-energy particles was registered during that period.

At ~0949 UT (~10 min after the F13 pass), the DMSP F14 satellite registered undulations with an amplitude of ~150 km and a wavelength of ~300 km (Fig. 5c). The average velocity of undulations estimated from Fig. 5b is ~800 m/s. A difference in the undulation velocity and drift velocity  $V_y$  (Fig. 5e) is apparently caused by the fact that the DMSP F13 trajectory did not pass exactly along the meridian. The undulation parameters estimated using the satellite data generally agree with the ground-based observations.

### 3. DISCUSSION

The analyzed event was unusual because the first large-scale undulations in the evening sector (~1700–1800 MLT) were registered within the diffuse zone of auroras. Many works on the satellite (see e.g., [Lui et al., 1982; Kelley, 1986; Yamamoto et al., 1993, 1994; Zhang et al., 2005]) and ground-based [Baishev et al., 1997, 2000] observations are devoted to studying large-scale undulations. These works studied undulations that were registered at the equatorward boundary of diffuse auroras. It is considered that undulations are the characteristic manifestation of magnetic storms. Our analysis indicated that large-scale undulations on December 12, 2004, were observed during enhancement of the two-vortex current system and magnetospheric convection as was previously reported in [Baishev et al., 1997, 2000].

The Kelvin–Helmholtz (K–H) instability is the most probable mechanism by which the generation of undulations is explained [Lui et al., 1982; Kelley,

1986]. This instability originates at a strong shear flow of plasma near the auroral oval equatorward boundary as a result of the appearance of intense northward electric fields. Such fields result in the origination of SAPSs [Foster and Burke, 2002]. During our event, SAPS is registered south of the diffuse aurora equatorward boundary in the region of the main ionospheric trough (see [Foster and Burke, 2002]).

According to the model calculations [Yamamoto et al., 1993, 1994], undulations can be identified with spatial modulation of energetic protons drifting in the magnetic field by Kelvin–Helmholtz waves. The K–H instability originates in the region of closed azimuthally extended layers with increased plasma density (arc sheets according to the author's terminology), localized equatorward of diffuse proton auroras. In the event considered by us, the regions of increased precipitation of keV electrons (Fig. 5) and generation of strong electric fields (Fig. 4) are localized within the diffuse auroral zone. The ionospheric data from Tixie Bay—the appearance of a slant  $E_s$  reflection on the ionogram at 0900 UT (Fig. 4)—testifies to the generation of strong electric fields.

Based on the DMSP data, Zhang et al. [2005] determined the necessary conditions for formation of undulations at the equatorward boundary of diffuse proton auroras: high-velocity ion drifts ( $>1000$  m/s) and a large their gradient ( $>0.1$  s $^{-1}$ ). In the event analyzed by us, the DMSP F15 observations (Fig. 5d) made it possible to determine the initial conditions of undulation generation: the drift velocity is  $V_y \sim 850$  m/s and the velocity gradient is  $\sim 0.08$  s $^{-1}$ . These values of the drift velocity and its gradient correspond to the values previously obtained in [Zhang et al., 2005].

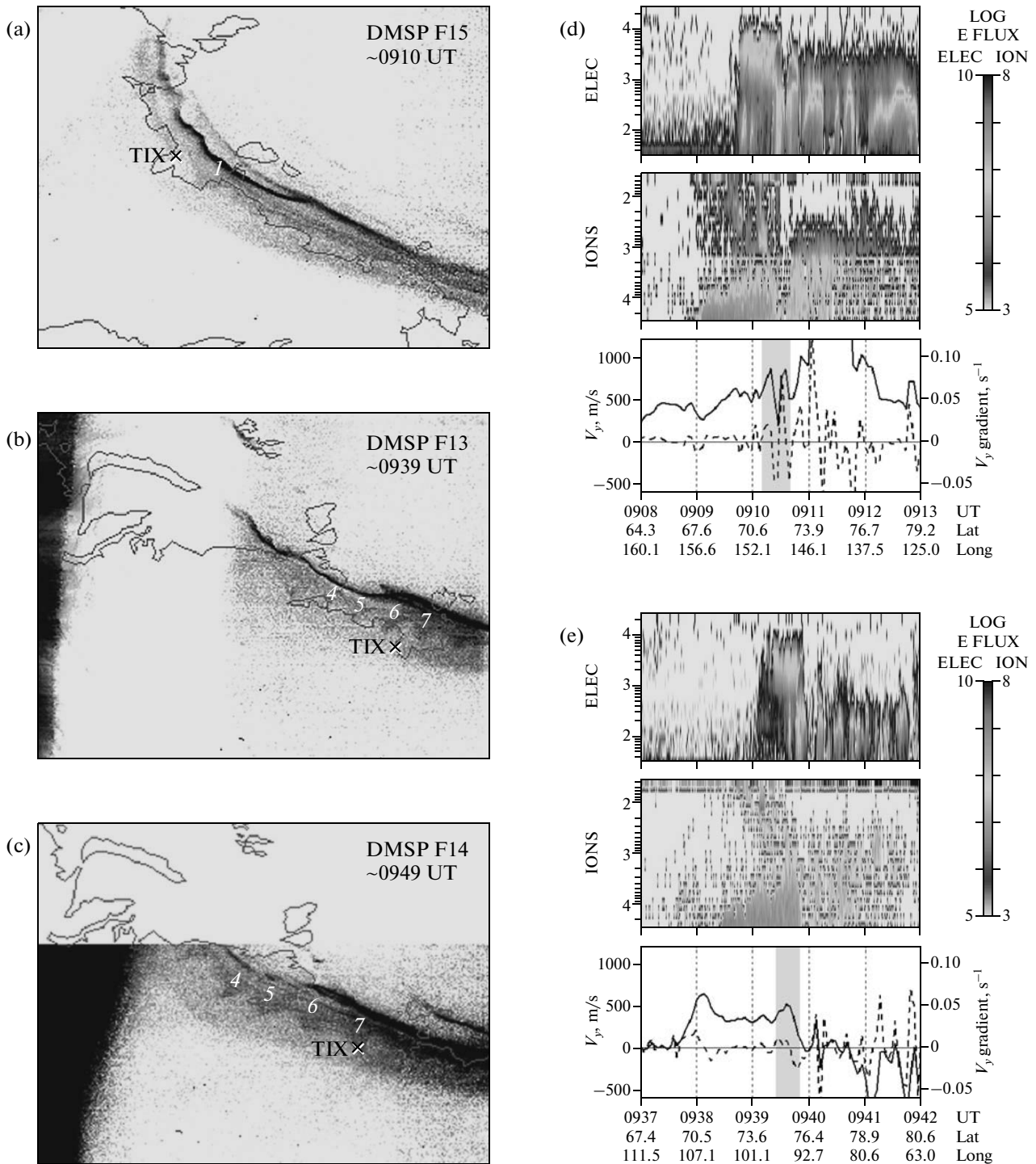


**Fig. 5.** The left-hand panels: aurora photographs from the DMSP satellites (a) F15, (b) F13, and (c) F14. The right-hand panels: the spectrograms of electron and proton precipitation, the variations in the horizontal drift velocity  $V_y$  (a solid line), and the velocity gradient (a dotted line) measured on the DMSP satellites (d) F15 and (e) F13, respectively. A gray rectangle marks the regions of formation of diffuse undulations.

#### 4. CONCLUSIONS

(1) Large-scale undulations in the evening sector ( $\sim 1700$ – $1800$  MLT) were for the first time registered

within the diffuse aurora zone. Eight undulations with an amplitude of  $\sim 100$ – $150$  km and a wavelength of  $\sim 200$ – $300$  km were registered at 0910–1000 UT on

December 12, 2004. The undulations propagated westward at a velocity of 0.7–0.8 km/s. The parameters of the undulations, registered during the TV observations agree with the DMSP satellite measurements.

(2) A comparison of the synchronous ground-based and satellite observations made it possible to determine the conditions of formation of large-scale undulations in the evening sector. High drift velocities ( $>800$  m/s) and a steep gradient of these velocities ( $>0.08$  s $^{-1}$ ) are the necessary conditions for generation of large-scale undulations. Strong electric fields are interrelated to the regions of increased precipitation of keV electrons.

### ACKNOWLEDGMENTS

We are grateful to T. Nagai and I. R. Mann for the presented Geotail and CARISMA magnetic data.

This work was supported by the Russian Foundation for Basic Research (project no. 09-05-98501-r\_vostok\_a) and partially by INTAS (grant 06-1000013-8823) and the Presidium of the Russian Academy of Sciences (Program 16, part 3).

### REFERENCES

- D. G. Baishev, E. S. Barkova, S. I. Solovyev, K. Yumoto, M. J. Engebretson, and A. V. Koustov, “Formation of Large-Scale, “Giant” Undulations at the Equatorial Boundary of Diffuse Aurora and Pc5 Magnetic Pulsations during the January 14, 1999 Magnetic Storm,” in *Proceedings of the Fifth International Conference on Substorms, St. Petersburg, 2000*, pp. 427–430.
- D. G. Baishev, K. Yumoto, S. I. Solovyev, N. E. Molochushkin, and E. S. Barkova, “Magnetic Storm-Time Variations of the Geomagnetic Field during Large-Scale Undulations of the Evening Diffuse Aurora,” *Geomagn. Aeron.* **37** (6), 39–46 (1997) [*Geomagn. Aeron.* **37**, 706–711 (1997)].
- B. E. Brunelli and A. A. Namgaladze, *Physics of the Ionosphere* (Nauka, Moscow, 1988) [in Russian].
- J. C. Foster and W. J. Burke, “SAPS: A New Categorization for Sub-Auroral Electric Fields,” *EOS Trans. AGU* **83** (36), 393–394 (2002).
- J. C. Foster and H. B. Vo, “Average Characteristics and Activity Dependence of the Subauroral Polarization Stream,” *J. Geophys. Res.* **107**, JA009409 (2002).
- M. C. Kelley, “Intense Sheared Flow as the Origin of Large-Scale Undulations of the Edge of the Diffuse Aurora,” *J. Geophys. Res.* **91**, 3225–3230 (1986).
- A. T. Y. Lui, C.-I. Meng, and S. Ismail, “Large Amplitude Undulations on the Equatorward Boundary of the Diffuse Aurora,” *J. Geophys. Res.* **87**, 2385–2400 (1982).
- J. K. Olesen, P. Stauning, and R. T. Tsunoda, “On a Unified Interpretation of the Polar Slant *E* Condition (SEC) and Other High *E* Field Related Phenomena,” *Radio Sci.* **21**, 127–140 (1986).
- K. Shiokawa, K. Yumoto, Y. Tanaka, et al., “Auroral Observations Using Automatic Instruments: Relations with Multiple Pi2 Magnetic Pulsations,” *J. Geomagn. Geoelectr.* **48**, 1407–1419 (1996).
- T. Yamamoto, K. Makita, and C.-I. Meng, “A Particle Simulation of “Giant” Undulations on the Evening Diffuse Auroral Boundary,” *J. Geophys. Res.* **98A**, 5885–5900 (1993).
- T. Yamamoto, M. Ozaki, S. Inoue, et al., “Convective Generation of “Giant” Undulations on the Evening Diffuse Auroral Boundary,” *J. Geophys. Res.* **99A**, 19499–19512 (1994).
- Y. Zhang, L. J. Paxton, D. Morrison, et al., “Undulations on the Equatorward Edge of the Diffuse Proton Aurora: TIMED/GUVI Observations,” *J. Geophys. Res.* **110**, A08211 (2005).